

## Simulation of water waves generated by a potential debris avalanche in Montserrat, Lesser Antilles

Philippe Heinrich, Anne Mangeney, Sandrine Guibourg, Roger Roche

Laboratoire de Détection et de Géophysique, Commissariat à l'Energie Atomique, France

Georges Boudon, Jean-Louis Cheminée

Institut de Physique du Globe, Paris, France

**Abstract.** The evolution of the volcano activity in Montserrat could lead to the collapse of a portion of the lava dome in the Tar River Valley and to a sudden entry of debris avalanche into the Caribbean Sea. The impact of a debris avalanche with a volume of  $40 \times 10^6 \text{ m}^3$  into the sea and the generated tsunami have been simulated numerically by a mixture model solving the 3D Euler's equations. The mixture is composed of sediments considered as an homogeneous fluid of density 2 and of water. Numerical tests show that the generated waves are sensitive to both initial impact velocities and avalanche fronts of the landslide. The water surface and velocities calculated by the 3D mixture model are used as input data in a non-linear shallow water model, to calculate tsunami propagation along the coasts of Montserrat. The hydraulic risks in Montserrat are roughly assessed for a tsunami generated by a mass of  $40 \times 10^6 \text{ m}^3$  entering the sea.

### 1. Introduction

Tsunamis generated by a sudden entry of debris avalanche resulting from gravitational failures of volcanic edifice into the sea have caused some of the worst natural disasters in historic times. The most well known events are the tsunamis associated with the 1883 eruption of Krakatau (Indonesia), the eruption of Mt. St. Augustine (Alaska) the same year and the collapse of the Unzen volcano (Japan) in 1792, creating a debris avalanche of  $300 \times 10^6 \text{ m}^3$ . The resulting tsunami of this latter event, with inundation heights of 6 to 10 meters at the shoreline, killed 15,000 people along the Shimabara Peninsula coastline and in the Ariake Sea [Francis, 1993].

The evolution of the volcanic activity at Soufriere Hills in Montserrat has led since 1995 to several debris avalanches reaching the sea [Young *et al.*, 1998]. On the 26th December 1997, a debris avalanche with an estimated volume of about  $40 \times 10^6 \text{ m}^3$  occurred in the White River valley, south of Montserrat. Evidence of associated large water waves was observed ashore at Old Road Bay, situated at a distance along the coast of 10 km NNW from the landslide area. Until now, only few data on this event are available [Calder *et al.*, 1998]. It has been then decided to study a similar scenario with a high probability of occurrence in the Tar River Valley, located in the horseshoe-shaped crater on the eastern flank of the volcano. This debris avalanche might lead to a tsunami propagating in the direction of Guadeloupe and Antigua, situated at about 50 km at the SE and NE of Montserrat, respectively.

Modeling of water waves generated by debris avalanches [Sander and Hutter, 1996] is still poorly understood and is generally based on two major assumptions. The first one concerns the generation mechanism, the second one the equations governing the water motion close to the impact. Most of the numerical models simulate the generation mechanism as the prescribed motion of the fluid domain boundaries. For instance, landslides are modeled by submerged or partly emerging pistons [Sander and Hutter, 1992, 1996], by a rigid triangular box impacting the water mass [Heinrich, 1992], or by an initial upward water displacement corresponding to the volume of a debris avalanche entering the sea [Nomanbhoy and Satake, 1995; Synolakis, 1997]. In all these cases, the interaction between debris avalanches and water is not taken into account. Furthermore, except for Heinrich [1992], the models simulating landslide-generated water waves are based on the shallow water assumption which appears to fail for most real events, in the area where the avalanche plunges into water [Sander and Hutter, 1992].

The two above-mentioned assumptions have been eliminated in this paper by developing a 3D model solving the Euler's equations for a mixture of two fluids. This model deals with the full interaction of debris avalanche and water, including the deformation of the entering mass. Sensitivity tests to initial conditions are investigated by varying the initial avalanche fronts and initial velocities of the mass entering the sea.

The hydraulic risks along the coasts of Montserrat are then roughly assessed for one of the studied test cases. The water waves calculated by the 3D mixture model are used as initial conditions in a standard non-linear shallow water model.

### 2. Numerical modeling of the debris avalanche impact into the sea

Fluid mechanics models are generally used to simulate subaerial or submarine landslides due to their observed fluid-like behaviors [Iverson, 1997; Jiang and Leblond, 1993; Sousa and Voight, 1995]. To simulate the interaction of the debris avalanche with the sea, we have developed a 3D model based on the Euler's equations where water and debris avalanche are considered as a mixture of two fluids. The 2D version of this numerical model has been validated by laboratory experiments consisting in the submarine slide of a gravel mass along an inclined plane [Assier *et al.*, 1997]. The main characteristic of mixture models is to deal with only one fluid with variable density in time and space. The mixture is composed here of sea water taken as a fluid of density  $\rho_1=1$  and of the debris material treated as an homogeneous fluid of density

Copyright 1998 by the American Geophysical Union.

Paper number 98GL01407.  
0094-8534/98/98GL-01407\$05.00

$\rho_2=2$ . The mixture density  $\rho$  is defined by the relation ( $\rho=(1-c)\rho_1+c\rho_2$ ), where  $c$  is the volume fraction of sediments. A unit value of  $c$  corresponds to a highly concentrated part of sediments and a 0 value of  $c$  indicates the water region.

At the origin time ( $t=0$ ), the debris avalanche is modeled by a parallelepiped of material with a volume of  $40 \times 10^6 \text{ m}^3$  in a U-shaped chute with a 800 m width and a slope of 10% (Figures 1 and 2). Three different heights  $H$  of the avalanche front are considered (15, 25 and 35 m) corresponding to the respective lengths  $L=3330, 2000$  and  $1430$  m. For each geometry, 4 initial velocities  $V$  (10, 25, 40 and  $55 \text{ ms}^{-1}$ ) have been studied. These values are in the range of calculated and observed debris avalanches of volcanic origin [e. g., *Sousa and Voight, 1995*] and are similar to those estimated for the 26 December 1997 landslide in Montserrat.

Our 3D model is based on the 3D hydrodynamics code of *Torrey et al. [1987]* developed for a single fluid. It solves the Euler's equations with a free-surface for a mixture of two incompressible fluids using an Eulerian finite-difference method. In this study, the debris avalanche is assumed to be a non-viscous fluid flowing down a frictionless slope and is considered to be non-porous while sliding into water. Moreover, friction between the two mediums is neglected. The non-linear governing equations of the mixture can be then written as follows :

$$\frac{\partial \rho}{\partial t} + \nabla \cdot (\rho \mathbf{v}) = 0 \quad (\text{continuity equation})$$

$$\frac{\partial \mathbf{v}}{\partial t} + \mathbf{v} \cdot \nabla \mathbf{v} = \mathbf{g} - \frac{\nabla p}{\rho} \quad (\text{momentum equation})$$

$$\frac{\partial F}{\partial t} + \nabla \cdot F \mathbf{v} = 0 \quad (\text{transport equation})$$

$$\nabla \cdot \mathbf{v} = \frac{\rho_2 - \rho_1}{\rho_1 \rho_2} \nabla \cdot \mathbf{j} \quad (\text{diffusion equation})$$

where  $\mathbf{v}$  is the 3D fluid velocity vector of the mixture;  $\mathbf{g}$  is the gravity acceleration;  $p$  is the pressure;  $\mathbf{j}$  is the diffusion flux and is set at 0, since no dilution of debris material into water is calculated;  $F$  is the fractional volume of the cell occupied by the mixture and is used to calculate the free-surface evolution. The model being Eulerian, the resolution of the continuity equation leads to the classical problem of numerical diffusion at the interface between water and debris flow. To suppress it, a method has been developed based on a donor-

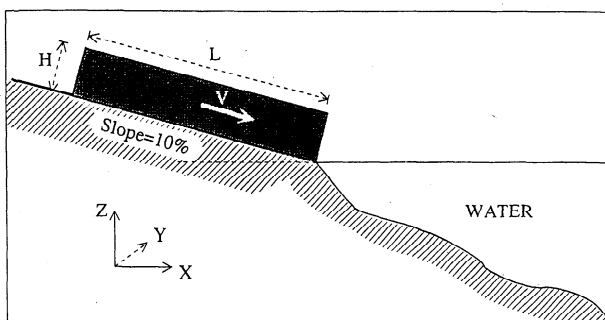


**Figure 1.** Sketch of the landslide geometry. The landslide contacts the still water surface at the time  $t=0$ s.

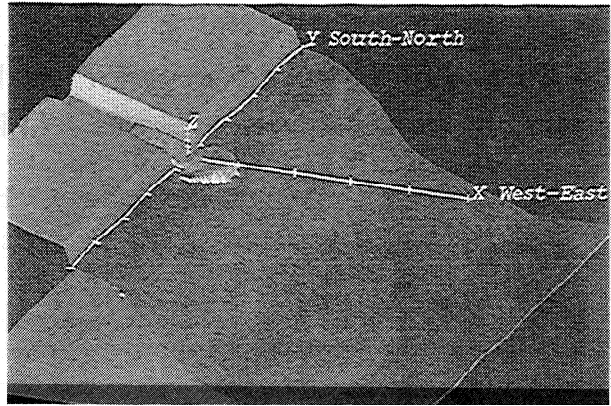


**Figure 2.** 3D computational domain. The vertical scale has been exaggerated by a factor of 3. The interval between ticks is 1000 m on the horizontal axis ( $x, y$ ) and 100 m on the vertical axis. The debris avalanche flows down a 800 m wide, U-shaped valley before impacting water.

acceptor technique. This technique is adapted from the one used by *Torrey et al. [1987]* for the convection of  $F$ . When no physical diffusion is calculated, as it is the case here, the convection of  $c$  from a donor cell to an empty downstream cell ( $c=0$ ) is carried out provided that the upstream donor cell is full ( $c=1$ ). This method allows one to follow the interface water-sediments without numerical diffusion.

The 3D computational domain is shown in Figure 2. The topography and bathymetry are assumed to be symmetric with respect to the axis of the Tar River valley (i. e.  $x$ -axis), modeled as a U-shaped, west-east orientated depression of 800 m wide. Both topography and bathymetry are uniform in the  $y$ -direction (i. e. south-north direction), excepted for the U-shaped valley. Due to the symmetry, numerical simulations are only carried out in the  $y>0$  domain. The 3D computational domain extends over 8 km from west to east in the  $x$ -direction, over 4.5 km from south to north in the  $y$ -direction and from -750 m to 400 m in the vertical direction. The mesh consists of  $100 \times 80$  cells in the horizontal directions and 60 cells in the vertical direction. The minimum horizontal grid increment is 50 m in the area of the Tar River delta over an area of  $1 \times 1 \text{ km}^2$ , the vertical grid increment is 5 m at the water surface and increases progressively upward and down to the bottom.

### 3. Results

The relative importance of the initial avalanche fronts and of the initial velocities is investigated by varying these parameters in 12 case studies (4 velocities and 3 front heights). To begin with, let us consider one of the numerical experiments, performed for a mass entering the sea at  $40 \text{ ms}^{-1}$  with a 25 m avalanche front. Figure 2 shows the large deformation undergone by the mass front interacting with water, 30 seconds after the origin time. The computed water surface is represented at  $t=50$  seconds on Figure 3. The water surface is composed of a leading elevation wave with an amplitude of about 20 meters located at 2 km from the coastline. It is followed by a trough of 40 meters close to the shore, created by the pushing action of the landslide. The trough amplitude is maximum at about  $t=50$  seconds before being filled in by the surrounding water. The waves propagate in a semi-circular fashion outside the slide area, with maximum wave heights occurring in the slide direction.

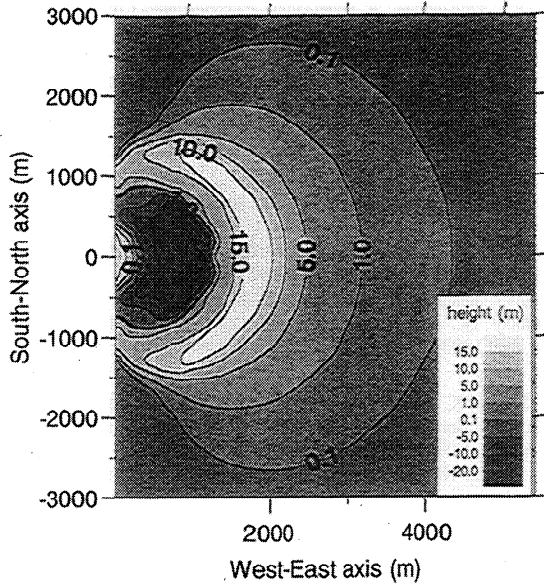


**Figure 3.** Tsunami generation by a landslide of  $40 \times 10^6 \text{ m}^3$  entering the sea at  $40 \text{ ms}^{-1}$  with an initial avalanche front of 25 m. Computed water surface, 50 seconds after the impact.

For the same experiment, time series of the computed surface elevation are presented at five different locations along the main direction of propagation (i. e. the  $x$ -axis) (Figure 4). Gauge 1 ( $x=0$ ) is located just at the valley mouth and is representative of the fluid height impacting the sea. Fluctuations around the initial value of 25 m occur during the first 50 seconds showing deformation of the mass due to its interaction with water. The whole mass penetrates into water within 60 seconds of the impact, the mean velocity of the landslide decreases slightly from  $40 \text{ m/s}$  to  $30 \text{ m/s}$  during this time interval. As the wave travels along the  $x$ -direction, the heights decrease rapidly due to geometric dispersion and increasing bathymetry (Figure 4).

For each of the 12 numerical experiments, it can be observed that the wave forms are similar to those observed in Figure 4. The set of numerical results shows also that the mean velocity of the mass penetrating into the sea decreases for initial velocities of  $55 \text{ ms}^{-1}$  and  $40 \text{ ms}^{-1}$ , whereas it increases for velocities lower than  $25 \text{ ms}^{-1}$ . For a same geometry, the mean velocities converge to the same terminal value when the whole mass has entered the sea. Figure 5 compares the maximum calculated water heights at a water depth of 600 m, 3 km from the impact location ( $x=3 \text{ km}$ ). Results show that the computed heights are strongly dependent on the avalanche front within the range of the studied values. Concerning the

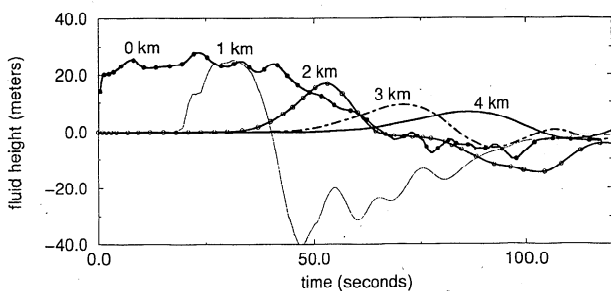


**Figure 4.** Same simulation as in Figure 3. Computed water wave elevations at 5 locations along the  $x$  axis ( $y=0$ ).

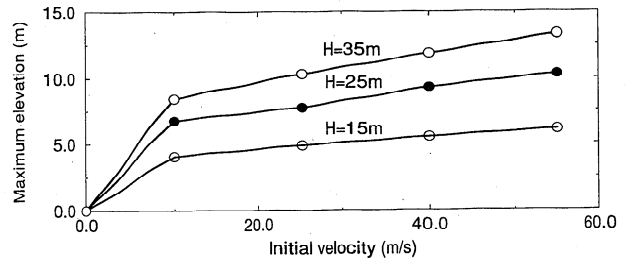


**Figure 5.** Comparisons between maximum calculated tsunami heights at a distance of 3 km from the impact location. The maximum heights of the 12 numerical experiments (represented by circles) are expressed as a function of the initial slide velocity. The 3 solid lines represent the 3 studied geometries.

dependence on initial velocities, the wave amplitudes seem to tend rapidly to asymptotic values. This result may be accounted for by the convergence of velocities for a same geometry; it is also confirmed by the laboratory tests of *Visher* [1986], showing that the plunge velocity is of secondary importance with respect to the maximum observed wave height.

#### 4. Tsunami propagation along Montserrat coasts

Due to the high numerical cost of 3D modeling, further propagation of the generated waves can not be calculated by the 3D model presented above.

Hence, the propagation is simulated by a standard shallow water model initialized by the results of the 3D model. The selected case is the numerical experiment with an impact velocity of  $40 \text{ ms}^{-1}$  and an avalanche front of 25 m. The nonlinear shallow water equations we solve, are referred to as 2+1 in the literature [*Titov and Synolakis, 1997*], indicating that there are two spatial horizontal propagation directions ( $x$  and  $y$ ) and one temporal ( $t$ ). The equations are solved by a finite differ-

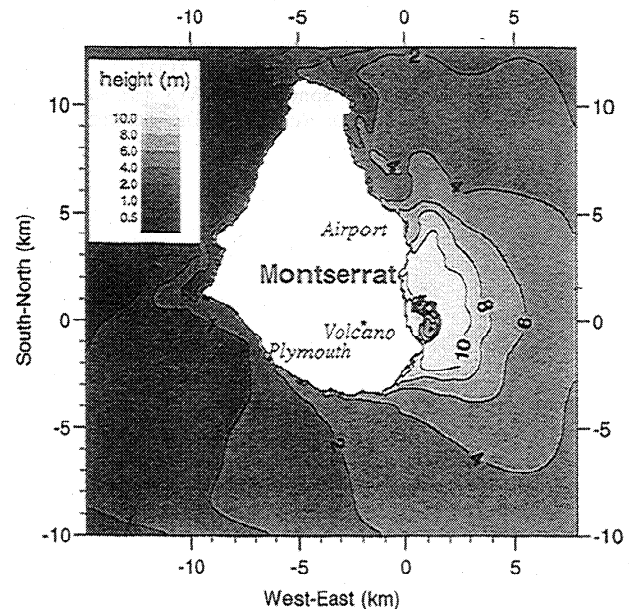


**Figure 6.** Maximum water surface elevation on Montserrat coasts reached during the tsunami propagation. This map is calculated by a shallow water model for a landslide of  $40 \times 10^6 \text{ m}^3$  flowing down the Tar River valley.

ence method, using an upwind scheme, iterative in time to limit the numerical oscillations due to non-linearities. Run-up is not simulated and complete reflection is calculated at a depth-contour of 10 meters. The computed domain extends over 25 x 25 km<sup>2</sup> with a grid space step of 100 meters.

Water wave heights and velocities used as initial conditions in the 2+1 model have to be calculated by the 3D model at times when most of the energy has been transferred from the landslide to water waves. It has been checked that initializations at  $t=40$ , 50 and 60 seconds give similar water heights along the coasts of Montserrat. For an initialization at  $t=50$  s, Figure 6 shows the maximum water surface elevation reached during the tsunami propagation. It has to be pointed out that the results along the coasts are underestimated due to the threshold-depth of 10 m [Titov and Synolakis, 1997] and due to the coarse grid resolution [Guibourg et al., 1997].

Figure 6 shows that most of the wave energy propagates in the open sea in the slide direction, i.e. towards Guadeloupe and Antigua. Along the coast, water heights of 1 to 2 meters are obtained at distances of about 10 km from the generation area.

## 5. Conclusion

A 3D mixture model is used to calculate water waves generated for a debris avalanche entering the sea. Water waves are propagated at further distances by a shallow water model. The calculated water heights along the Montserrat coast are in the range of those estimated for a similar event that occurred on the 26th of December, 1997 at Old Town.

**Acknowledgments.** The authors are grateful to Dr. Yves Caristan, President of the Comité Supérieur d'Évaluations des Risques Volcaniques in France and Dr. J. Bouchez, head of the Laboratory of Detection and Geophysics, CEA, France for their support. The authors would like also to thank the Montserrat Volcano Observatory and the Guadeloupe Volcano Observatory for providing bathymetric data.

## References

- Assier, S., C. Mariotti, and Ph. Heinrich, Numerical simulation of submarine landslides and their hydraulic effects, *J. Wtrwy., Port, Coast., and Oc. Engrg., ASCE*, 123, 149-157, 1997.
- Calder E., S. Young, R. Steve, J. Sparks, and MVO staff, *Montserrat Volcano Observatory, Special Report 06*, The Boxing day collapse, 1998.
- Francis, P., *Volcanoes, A Planetary Perspective*, Oxford University Press Inc., NY, 1993.
- Guibourg, S., Ph. Heinrich, and R. Roche, Numerical modeling of the 1995 Chilean tsunami. Impact on French Polynesia, *Geophys. Res. Lett.*, 24, 775-778, 1997.
- Heinrich, Ph., Nonlinear water waves generated by submarine and aerial landslides, *J. Wtrwy., Port, Coast., and Oc. Engrg., ASCE*, 118, 249-266, 1992.
- Iverson, R. M., The physics of debris flows, *Rev. Geophys.*, 35, 245-296, 1997.
- Jiang, L., and P.H. Leblond, Numerical modeling of an underwater Bingham plastic mudslide and the waves which it generates, *J. Geophys. Res.*, 98, 304-317, 1993.
- Nomanbhoj, N., and K. Satake, Generation mechanism of tsunamis from the 1883 Krakatau eruption, *Geophys. Res. Lett.*, 22, 509-512, 1995.
- Sander, J., and K. Hutter, Evolution of weakly non-linear channelized shallow water waves generated by a moving boundary, *Acta Mech.*, 91, 119-155, 1992.
- Sander, J., and K. Hutter, Experimental and computational study of channelized water waves generated by a porous body, *Acta Mech.*, 115, 133-149, 1996.
- Sousa, J., and B. Voight, Multiple pulsed debris avalanche emplacement at Mount St. Helens in 1980: Evidence from numerical continuum flow simulations, *J. Volcanology and Geothermal Res.*, 66, 227-250, 1995.
- Synolakis, C.E., Ph. Liu, G. Carrier, and H. Yeh, Tsunamigenic sea-floor deformations, *Science*, 278, 598-600, 1997.
- Titov, V.V., and C.E. Synolakis, Extreme inundation flows during the Hokkaido-Nansei-Oki tsunami, *Geophys. Res. Lett.*, 24, 1315-1318, 1997.
- Torrey, M.D., R.C. Mjolsness, and L.R. Stein, Nasa-Vof3D: a three-dimensional computer program for incompressible flows with free surfaces, *Report LA11009-MS*, Los Alamos National Laboratory, 1987.
- Visher, D.L., Rockfall-induced waves in reservoirs, *Water Power and Dam Construction*, 45-48, Sept. 1986.
- Young, S., R. Robertson, Lynch, Miller, Ambeh, Aspinall, Shepherd, Sparks and MVO staff, Overview of the volcano and the eruption with a chronology, *Geophys. Res. Let. (This volume)*
- Ph. Heinrich, A. Mangeney, S. Guibourg and R. Roche, Laboratoire de Détection et de Géophysique, Commissariat à l'Énergie Atomique, B.P. 12, 91680 Bruyères-le-Châtel, France.  
(email : heinrich@ldg.bruyeres.cea.fr)
- G. Boudon, J.L. Cheminee, Observatoires Volcanologiques, Institut de Physique du Globe de Paris, Tour 24, Case 89, 4, Place Jussieu, 75252 Paris Cedex 05, France (email : boudon@ipgp.jussieu.fr; cheminee@ipgp.jussieu.fr)

(Received November 5, 1997; revised February 12, 1998; accepted April 14, 1998)